Journal of Alloys and Compounds 525 (2012) 58–62

Contents lists available at SciVerse ScienceDirect

Journal of Alloys and Compounds

journal homepage: www.elsevier.com/locate/jallcom

Spectroscopic and magnetic behavior of Gd and Nd ions in lead–germanate glasses

Lidia Pop, Maria Bosca, Eugen Culea*

Technical University of Cluj-Napoca, Memorandumului 28, 400114, Cluj-Napoca, Romania

ARTICLE INFO

Article history:
Received 13 October 2011
Received in revised form 7 February 2012
Accepted 8 February 2012
Available online xxx

PACS:
61.43.Fs, 75.50.Lk, 07.57.−c, 75.30.Cr

Keywords:
Glasses
Rare earth
Spectroscopy
Magnetic susceptibility

ABSTRACT

Samples of the $x\mathrm{Gd_2O_3}(1-x)[\mathrm{GeO{\cdot}PbO}]$ and $x\mathrm{Nd_2O_3}(1-x)[\mathrm{GeO{\cdot}PbO}]$ vitreous systems with $0 \le x \le 0.15$ were prepared and investigated by X-ray diffraction, FTIR spectroscopy and magnetic susceptibility measurements (in addition, the samples containing gadolinium ions were investigated by electron paramagnetic resonance (EPR) spectroscopy). FTIR spectroscopy investigation shows that the studied samples consist of both $\mathrm{GeO_4}$ and $\mathrm{GeO_6}$ structural units, the $\mathrm{GeO_4}$ being predominant. The increase of the gadolinium or neodymium ion content of the samples determines the $\mathrm{GeO_4} \to \mathrm{GeO_6}$ conversion process. FTIR data suggest that the rare earth ions present in the vitreous matrix play a network modifier role. Magnetic susceptibility data show that the magnetic behavior of the studied samples is due to the presence of the $\mathrm{Gd^{3+}}$ and $\mathrm{Nd^{3+}}$ ions. These ions appear as isolated species for low rare earth oxide contents, $x \le 0.03$–0.05, while for higher contents appear as magnetically coupled species, too.

EPR spectroscopy data obtained for the $x\mathrm{Gd_2O_3}(1-x)[\mathrm{GeO_2{\cdot}PbO}]$ samples show that, in addition to the network modifier role of the rare earth ions suggested by the FTIR data, the $\mathrm{Gd^{3+}}$ ions play also the network former role.

1. Introduction

In the last years lead–germanate glasses have received much attention due to their important properties such as a good chemical durability and mechanical stability, high glass transition temperature, higher laser damage thresholds at 3 μm, etc. [1–6]. Lead–germanate vitreous systems offer possibilities for various applications in optoelectronics and telecommunication technology and are suitable for waveguide applications since, for the IR region, they are low loss optical materials. Moreover, lead–germanate glasses can be easily obtained into fiber form and this enhances their status as materials of particular interest for telecommunications. [7,8]

On the other hand, glasses and crystals containing rare earth (RE) ions have attracted great attention since the addition of these ions [7–10], as well as the addition of the transition metal ions [11–15], generate important properties for the host matrix. Such materials present extensive applications in fields such as information display and laser technology [7–10]. Glasses containing neodymium ions are intensively used in laser technology [10]. Gadolinium ions are known for their capacity to be incorporated in vitreous matrices in high amounts offering thus important information concerning the compositional structural evolution of the host glass, their magnetic interaction and their clusterization process [i.e., 16–20].

In order to obtain more information concerning the important class of lead–germanate glasses doped with rare earth ions, in the present paper we studied some structural and magnetic properties of neodymium and gadolinium ions immobilized in the $\mathrm{GeO_2{\cdot}PbO}$ vitreous matrix. The effect of the progressive addition of RE ions on the structural and physical properties of the $\mathrm{GeO_2{\cdot}PbO}$ host matrix was followed by means of X-ray diffraction, FTIR spectroscopy, magnetic susceptibility and electron paramagnetic resonance (EPR) spectroscopy measurements.

2. Experimental

Samples of the $x\mathrm{Gd_2O_3}(1-x)[\mathrm{GeO{\cdot}PbO}]$ and $x\mathrm{Nd_2O_3}(1-x)[\mathrm{GeO{\cdot}PbO}]$ systems where $x = 0$, 0.01, 0.05, 0.10 and 0.15, were prepared by the melt quenching method. Required quantities of analar grade $\mathrm{GeO_2}$, PbO and $\mathrm{Nd_2O_3}$ or $\mathrm{Gd_2O_3}$ oxides were mixed and milled together with the aim to obtain a fine powder. The mixture was melted in sintered corundum crucibles in an electric furnace at a temperature of 1200 °C for 10 min. The samples were obtained by pressing the melts between two steal plates. Taking into account the important dependence of the structure and properties of the vitreous systems on their "thermal history" and in order to offer a reasonable comparative study of the investigated systems, all the samples were prepared strictly under the same conditions.

X-ray diffraction investigation was performed using a XRD-6000 Shimadzu diffractometer with a graphite monochromator for the Cu Kα radiation ($\lambda = 1.54$ Å) at room temperature. X-ray diffraction confirmed the amorphous nature of the samples.

The FTIR investigation was performed using a JASCO FT-IR 6200 spectrometer. The FTIR spectra were recorded in the 400–1800 cm^{-1} range at room temperature,

---

* Corresponding author. Tel.: +40 264 401536; fax: +40 264 595355.
E-mail address: eugen.culea@phys.utcluj.ro (E. Culea).

0925-8388/$ – see front matter © 2012 Elsevier B.V. All rights reserved.
doi:10.1016/j.jallcom.2012.02.069

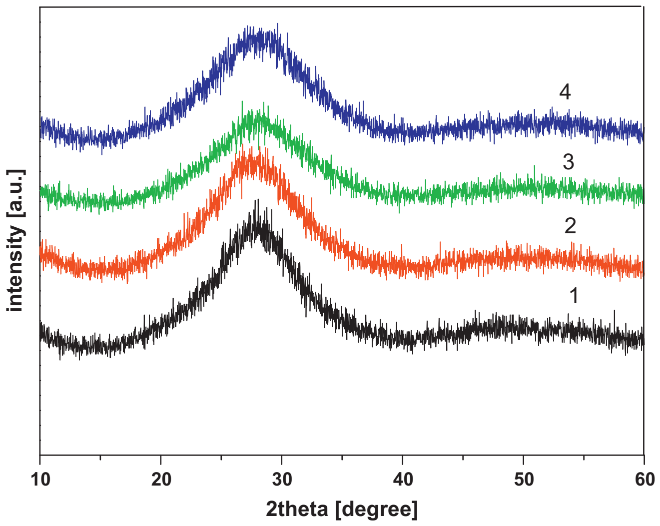

Fig. 1. X-ray diffractograms of the $0.05Gd_2O_3{\cdot}0.95(GeO_2{\cdot}PbO)$ (1), $0.05Nd_2O_3{\cdot}0.95(GeO_2{\cdot}PbO)$ (2), $0.15Gd_2O_3{\cdot}0.85(GeO_2{\cdot}PbO)$ (3) and $0.15Nd_2O_3{\cdot}0.85(GeO_2{\cdot}PbO)$ (4) glasses.

using the KBr pellet technique. In order to obtain good quality spectra the samples were crushed in an agate mortar to obtain a fine powder.

The magnetic susceptibility measurements were performed using a Faraday-type balance in the 80–300 K temperature range. The sensitivity of the equipment was 10^{-7} emu/g. The diamagnetic susceptibility of the GeO_2 base glass was measured, too, and the magnetic susceptibility data for all the samples were corrected taking into account the diamagnetic contribution of the host matrix.

EPR spectra were recorded using an Adani PS8400 spectrometer. The measurements were performed in the X band at room temperature.

3. Results and discussion

Fig. 1 presents the X-ray diffractograms for some of the $xGd_2O_3(1-x)[GeO{\cdot}PbO]$ and $xNd_2O_3(1-x)[GeO{\cdot}PbO]$ samples.

The X-ray diffractograms highlight the amorphous nature of all the studied samples. Thus, the X-ray patterns exhibit a broad diffuse scattering at low angles confirming a long-range structural disorder characteristic of the amorphous network.

In order to determine the main features concerning the local structure of the studied glasses, FTIR absorption measurements were carried out since IR spectroscopic data provide important information concerning the local structure. FTIR spectra of the the $xGd_2O_3(1-x)[GeO{\cdot}PbO]$ and $xNd_2O_3(1-x)[GeO{\cdot}PbO]$ vitreous systems are shown in Fig. 2(a-Gd, b-Nd).

The absorption bands present in these IR spectra are very broad and asymmetric due to the amorphous nature of the samples. Due to this fact, in order to perform a reasonable analysis of the experimental IR data, a deconvolution procedure of the spectra was necessary. This procedure was performed with the Spectra Manager program using a Gaussian type function. Fig. 3 shows the deconvolution in Gaussian bands of the spectrum for the $GeO_2{\cdot}PbO$ host glass matrix.

The deconvolution procedure allowed a better identification of the IR bands that appear in the experimental spectra and offered the possibility to follow more precisely their compositional evolution. The locations of the most important IR absorption bands and their assignments are summarized in Table 1. The assignments were made based on data from the literature concerning some related vitreous or crystalline compounds [21–32].

The analysis of the IR data obtained for the studied systems suggests that the vitreous matrix of these glasses is built up of GeO_4, GeO_6 and PbO_4 structural units. This is suggested by the presence of the IR absorption bands located at 690–700 cm^{-1} (due to the symmetrical stretching vibrations of Ge—O—Ge bonds from

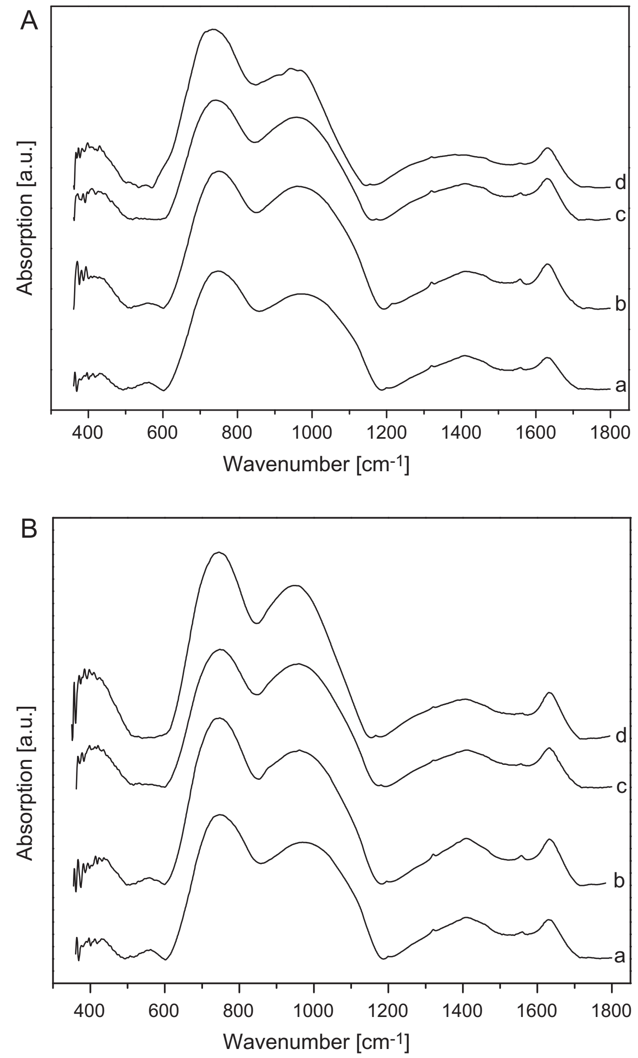

Fig. 2. IR spectra of the $xGd_2O_3(1-x)(GeO_2{\cdot}PbO)$ (A) and $xNd_2O_3(1-x)(GeO_2{\cdot}PbO)$ (B) glasses with $x = 0$ (a), $x = 0.05$ (b), $x = 0.10$ (c) and $x = 0.15$ (d).

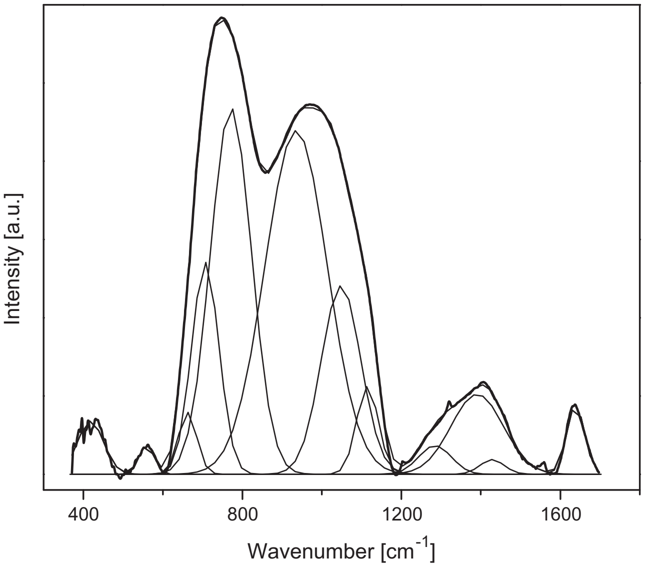

Fig. 3. Deconvolution of the IR spectrum for the $GeO_2{\cdot}PbO$ glass.

Table 1
FTIR absorption bands and their assignment for the $x\mathrm{RE_2O_3}(1-x)[0.95(\mathrm{GeO_2{\cdot}PbO}){\cdot}0.05\mathrm{Al_2O_3}]$ glasses where RE = Gd and Nd.

Wavenumber [cm^{-1}]	Assignments
413–426	Deformation vibrations for Pb—O bonds from $\mathrm{PbO_4}$ structural units [21].
	Deformations vibrations of Gd—O or Nd—O bonds [22,23].
550–558	Symmetrical stretching vibrations of Ge—O—Ge bonds [23,24].
	Asymmetrical deformation vibrations of Pb—O—Pb bonds [22].
690–700	Symmetrical stretching vibrations of Ge—O—Ge bonds from the $\mathrm{GeO_6}$ structural units [23,26–30].
757–782	Asymmetric stretching mode of Ge—O—Ge bridges connecting $\mathrm{GeO_4}$ units [24,26–30].
870–875	Asymmetrical stretching vibrations of Ge—O—Ge bonds from the $\mathrm{GeO_4}$ units [23–30].
965	Symmetrical stretching vibrations of Pb—O [21].
1045–1050	Asymmetrical stretching vibrations of Pb—O [21].
	Ge—O stretch in GeO4 units [28,29].
1265	Deformations vibrations of Pb—O—Ge [32].
1395	Asymmetrical stretching vibrations of Ge—O—Ge [33].
1635	Deformations vibrations for OH [33].

the $\mathrm{GeO_6}$ structural units [23,26–30]), 870–875 cm^{-1} (due to the asymmetrical stretching vibrations of Ge—O—Ge bonds from the $\mathrm{GeO_4}$ structural units [23,26–30]) and 413–426 cm^{-1} (due to the symmetrical deformation vibrations of Pb—O bonds from $\mathrm{PbO_4}$ structural units [21]).

The addition of the RE ions (gadolinium and neodymium) produces some modifications of the IR features suggesting a compositional evolution of the structure for the studied vitreous matrices takes place. Thus, the increase of the RE ions content of the samples increases the intensity of the absorption band from 690 to 700 cm^{-1} and decreases that of the absorption band from 870 to 875 cm^{-1} suggesting the increase of the number of $\mathrm{GeO_6}$ structural units, respectively the decrease of the number of the $\mathrm{GeO_4}$ units. Since the $\mathrm{GeO_6}/\mathrm{GeO_4}$ ratio highly influences the properties of the $\mathrm{GeO_2{\cdot}PbO}$ glass matrix, our attention was focused on the compositional evolution of this ratio. In order to determine the $\mathrm{GeO_6}/\mathrm{GeO_4}$ ratio it was taken into account that each IR band is related to some type of vibration in specific structural groups and that the concentration of the structural group is proportional to the area of its characteristic IR band. We note that the deconvolution process makes it possible to obtain accurate values of the area of each IR absorption band. In order to express the $\mathrm{GeO_6}/\mathrm{GeO_4}$ ratio we note that it is proportional to the ratio of the areas of the absorption bands from 690 to 700 cm^{-1} and 870 to 875 cm^{-1}, A_6 and A_4. The compositional dependence of the A_6/A_4 ratio is shown in Fig. 4

The data from Fig. 4 show that for all the studied samples the amount of $\mathrm{GeO_4}$ structural unit present in the vitreous matrix of the samples is higher than that of the $\mathrm{GeO_6}$ unit. The plot from Fig. 4 shows that the increase of the RE oxide content of the samples up to $x = 0.15$ determines a $\mathrm{GeO_4} \rightarrow \mathrm{GeO_6}$ conversion process.

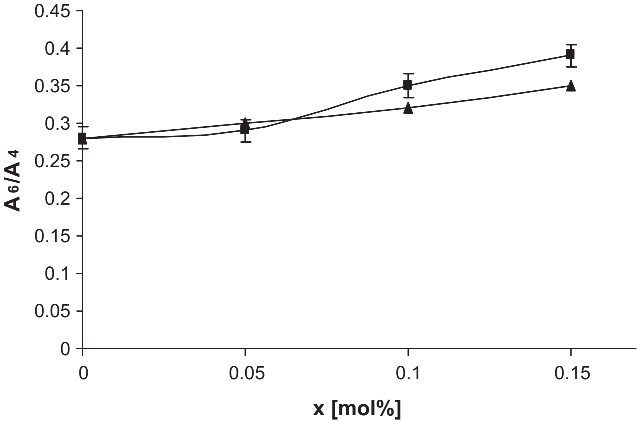

Fig. 4. Compositional evolution of the A_6/A_4 ratio for the $x\mathrm{Gd_2O_3}(1-x)(\mathrm{GeO_2{\cdot}PbO})$ (▲) and $x\mathrm{Nd_2O_3}(1-x)(\mathrm{GeO_2{\cdot}PbO})$ (■) glasses.

The absorption band located at about 1395 cm^{-1} becomes broader with increasing the rare earth oxide content, x, of the samples. This may suggest that the deformation degree of the germanium containing structural units increases with increasing x.

The structural modifications generated by increasing the RE oxide content confirm that in the studied $x\mathrm{Gd_2O_3}(1-x)[\mathrm{GeO{\cdot}PbO}]$ and $x\mathrm{Nd_2O_3}(1-x)[\mathrm{GeO{\cdot}PbO}]$ vitreous systems the gadolinium and neodymium ions play the network modifier role as was previously reported for other oxide glasses, too [i.e., 33,34].

The magnetic behavior of the $x\mathrm{Gd_2O_3}(1-x)[\mathrm{GeO{\cdot}PbO}]$ and $x\mathrm{Nd_2O_3}(1-x)[\mathrm{GeO{\cdot}PbO}]$ vitreous systems is due to the RE ions located in these glasses since the host glass matrix was found to be diamagnetic. As was previously reported, the gadolinium and neodymium ions appear in the oxide vitreous matrices in a single and stable valence state, namely the $\mathrm{Gd^{3+}}$ ($7.94\mu_B$) and $\mathrm{Nd^{3+}}$ ($3.627\mu_B$), where the values in the brackets represent the effective magnetic moments per free magnetic rare earth ion [10,35].

For the $x\mathrm{Gd_2O_3}(1-x)[\mathrm{GeO{\cdot}PbO}]$ and $x\mathrm{Nd_2O_3}(1-x)[\mathrm{GeO{\cdot}PbO}]$ vitreous systems studied in this paper, the temperature dependence of the magnetic susceptibility follows a Curie type magnetic behavior for low RE oxide contents ($x \leq 0.03$–0.05, the value differs depending on the type of RE ions) and a Curie-Weiss type one for higher RE contents. Such a behavior is characteristic of glasses containing RE ions being previously reported for several other oxide glasses containing RE ions [i.e., 36–40].

Magnetic susceptibility data obtained for the studied glasses were used to determine some important parameters such as the paramagnetic Curie temperature (θ_p), the molar Curie constant (C_M) and the effective magnetic moment per RE ion (μ_{eff}) for the studied glasses. We mention that the magnetic data were corrected taking into account the diamagnetic contribution of the host glass matrix. Fig. 5 presents the compositional variation of the paramagnetic Curie temperature, θ_p.

We note that θ_p is a rough indicator of the magnetic interactions between the magnetic ions from the studied glasses. Thus, in the frame of the molecular field model [41], the molecular field constant is given by $J \approx 2N_cJ_{ij}/Ng^2\mu_B{}^2 \approx \theta_p/C$ where N is the total number of magnetic ions, N_c is the number of exchange coupled magnetic ions, g is the spectroscopic splitting factor, μ_B is the Bohr magneton and J_{ij} is the exchange interaction between the magnetic ions. In this view, the zero values for θ_p suggest that the magnetic RE ions appear in the host vitreous matrix only as isolated species, while the values different from zero suggest that magnetic ions are present as both isolated and coupled species. Fig. 5 shows that the values measured for the θ_p were zero for very low RE contents ($x \leq 0.03$–0.05) and small and negative for higher RE contents. The fact that the θ_p parameter becomes different from zero for very low RE contents indicates an accentuated clustering tendency of the magnetic rare earth ions. The small and negative values of θ_p suggest the presence of weak antiferromagnetic interactions between

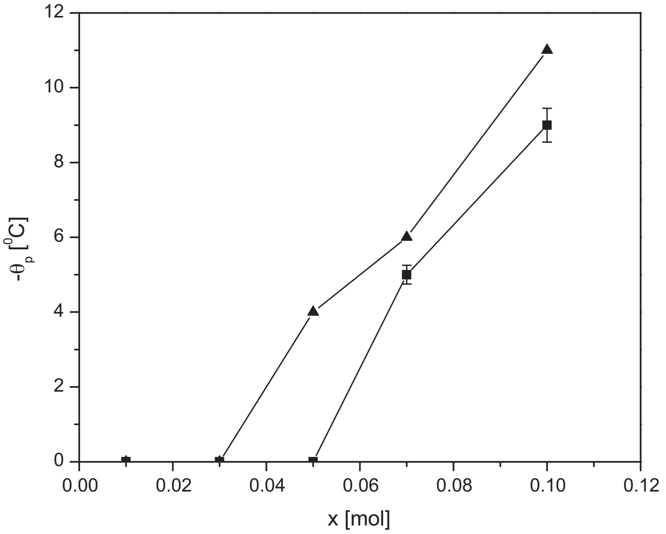

Fig. 5. Compositional evolution of the paramagnetic Curie temperatures for the $x\mathrm{Gd_2O_3}(1-x)(\mathrm{GeO_2{\cdot}PbO})$ (▲) and $x\mathrm{Nd_2O_3}(1-x)(\mathrm{GeO_2{\cdot}PbO})$ (■) glasses.

the magnetic RE ions located in the host vitreous matrix. Previous reports stated that the magnetic RE ions from vitreous matrices are coupled via RE–O–RE superexchange interactions [i.e., 16,42].

Fig. 6 presents the compositional variation of the effective magnetic moment per RE ion (μ_{eff}) for the studied glasses.

The analysis of the data from Fig. 6 shows that the μ_{eff} values are close but somewhat smaller than those for the free ions in the case of the gadolinium and neodymium ions. This suggests that the magnetic RE ions are present in their $\mathrm{Gd^{3+}}$, respectively $\mathrm{Nd^{3+}}$ valence states, and their magnetic interactions are weak and of antiferromagnetic nature.

For the samples containing gadolinium ions, $x\mathrm{Gd_2O_3}(1-x)[\mathrm{GeO{\cdot}PbO}]$, an EPR spectroscopy study was performed. The obtained EPR spectra are close to those of the $\mathrm{Gd^{3+}}$ ions located in lead–bismuthate glasses [40]. Thus, for $x \le 0.10$, the spectra show four resonance lines located at $g \approx 2$, 2.9, 4.9 and 5.9. This represents a superposition of two types of spectra due to the $\mathrm{Gd^{3+}}$ ions located in vitreous matrices. First, there is the well known "U" spectrum composed of the absorption signals from $g \approx 2$, 2.9 and 5.9, assigned to the $\mathrm{Gd^{3+}}$ ions located at sites with weak crystalline fields of different symmetries (tetrahedral, octahedral and cubic with moderate distorsions) having coordination numbers higher than 6 [38,40,43,44]. Second, there is the asymmetric absorption from $g \approx 4.9$ due to the $\mathrm{Gd^{3+}}$ ions located at sites with relatively strong crystal fields having an orthorhombic symmetry and coordination numbers lower than 6 [38,40]. This location of the $\mathrm{Gd^{3+}}$ ions is unusual since the general tendency of the RE ions is to be associated with high coordination numbers. However, such a location may appear in the studied $x\mathrm{Gd_2O_3}(1-x)[\mathrm{GeO{\cdot}PbO}]$ glasses when the $\mathrm{Gd^{3+}}$ ions replace the glass former germanium and/or lead ions. In this case, the EPR data suggest that the gadolinium ions play not only the glass modifier role proved by the IR data, but also the glass former role. Such a behavior of the $\mathrm{Gd^{3+}}$ ions was previously reported for the lead–bismuthate glasses [40].

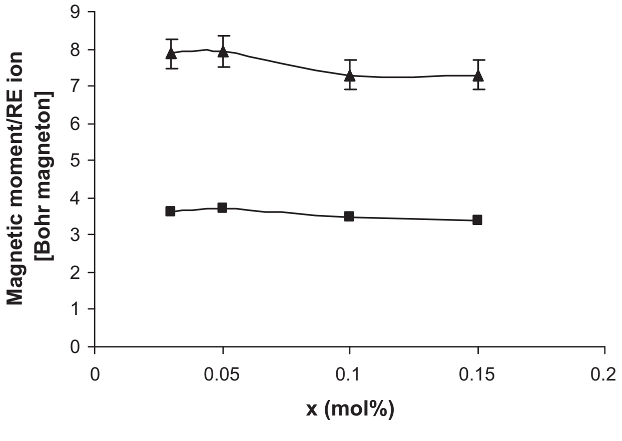

Fig. 6. Compositional variation of the effective magnetic moment per RE ion (μ_{eff}) for the $x\mathrm{Gd_2O_3}(1-x)(\mathrm{GeO_2{\cdot}PbO})$ (▲) and $x\mathrm{Nd_2O_3}(1-x)(\mathrm{GeO_2{\cdot}PbO})$ (■) glasses.

For higher gadolinium contents ($x > 0.10$) the EPR spectra consists of a single broad absorption line located at $g \approx 2$ associated with $\mathrm{Gd^{3+}}$ ions present predominantly as clustered species. We mention that the results of the EPR investigation agree with the magnetic susceptibility data.

4. Conclusions

Samples of the $x\mathrm{Gd_2O_3}(1-x)[\mathrm{GeO_2{\cdot}PbO}]$ and $x\mathrm{Nd_2O_3}(1-x)[\mathrm{GeO_2{\cdot}PbO}]$ $x \le 0.15$ were prepared and investigated. X-ray diffraction investigation shows that the samples containing gadolinium and neodymium ions were vitreous.

FTIR spectroscopy investigation shows that the studied samples consist mainly of $\mathrm{GeO_4}$ structural units but $\mathrm{GeO_6}$ units are present, too. The increase of the RE oxide content of the samples up to $x = 0.15$ determines a $\mathrm{GeO_4} \rightarrow \mathrm{GeO_6}$ conversion process. FTIR data suggest that the RE ions present in the vitreous matrix play the network modifier role.

Magnetic susceptibility data show that the magnetic RE ions ($\mathrm{Gd^{3+}}$, $\mathrm{Nd^{3+}}$) are present as isolated species only for very low contents ($x \le 0.03$–0.05). For higher x values the magnetic RE ions present exchange interactions of antiferromagnetic nature.

EPR spectroscopy data show that the $\mathrm{Gd^{3+}}$ ions play not only the network modifier role but also the network former one.

Acknowledgment

The financial support of the Ministry of Education and Research of Romania-National University Research Council (CNCSIS, PN II-IDEI 183/2008, contract number 476/2009) is gratefully acknowledged by the author.

References

[1] Z. Yang, S. Xu, L. Hu, Z. Jiang, J. Alloys Compd. 370 (2004) 94.
[2] W.A. Pisarski, Ł. Grobelny, J. Pisarska, R. Lisiecki, W. Ryba-Romanowski, J. Alloys Compd. 509 (2011) 8088.
[3] V.A. Kolesova, Fiz. Khim. Stekla 5 (1980) 325.
[4] J.E. Canale, R.A. Condrate St, K. Nassau, B.C. Cornilsen, J. Can. Ceram. Soc. 55 (1986) 50.
[5] S.J.L. Ribeiro, J. Dexpert-Ghys, V.R. Mastelaro, J. Non-Cryst. Sol. 159 (1993) 213.
[6] S.J.L. Ribeiro, F. Gilberto, de Sa, J. Brazil. Chem. Soc. 5 (1994) 77.
[7] M. Wachtler, A. Speghini, K. Gatterer, H.P. Fritzer, D. Ajo, M. Bettinelli, J. Am. Ceram. Soc. 81 (2005) 2045.
[8] N.S. Hussain, Y.P. Reddy, S. Buddhudu, Mater. Lett. 53 (2002) 25.
[9] W. Wang, J. Ren, D. Chen, S. Yuan, G. Chen, J. Alloys Compd. 516 (2012) 1.
[10] A. Flórez, E.M. Ulloa, R. Cabanzo, J. Alloys Compd. 488 (2009) 606.
[11] Y.B. Saddeek, E.R. Shaaban, K.A. Aly, I.M. Sayed, J. Alloys Compd. 478 (2009) 447.
[12] A.R. Molla, R.P.S. Chakradhar, C.R. Kesavulu, J.L. Rao, S.K. Biswas, J. Alloys Compd. 512 (2012) 105.
[13] A. Ghosh, J. Appl. Phys. 65 (1989) 227.
[14] S. Bhattacharya, A. Ghosh, Phys. Rev. B 68 (2003) 224202.
[15] N.A. Ghoneim, H.A. ElBatal, A.M. Abdelghany, I.S. Ali, J. Alloys Compd. 509 (2011) 6913.
[16] E. Culea, A. Pop, I. Cosma, J. Magn. Magn. Mater. 157 (1996) 163.
[17] S. Rada, M. Culea, M. Rada, T. Rusu, E. Culea, J. Alloys Compd. 490 (2010) 270.
[18] G. Zhang, M.J. Poulain, J. Alloys Compd 275–277 (1998) 15.
[19] S. Bhattacharya, A. Ghosh, Phys. Rev. B 70 (2004) 172203.
[20] S. Mandal, A. Ghosh, J. Phys.: Condens. Matter 8 (1996) 829.
[21] G.L.J. Trettenhahn, G.E. Nauer, A. Neckel, Vib. Spectrosc. 5 (1993) 85.

[22] L.M. Sharaf El-Deen, M.S. Al Salhi, M.M. Elkholy, J. Alloys Compd. 465 (2008) 333.
[23] E.I. Kamitsos, A.P. Patsis, M.A. Karakassides, G.D. Chryssikos, J. Non-Cryst. Solids 126 (1990) 52.
[24] E. Culea, L. Pop, M. Bosca, J. Alloys Compd. 505 (2010) 754.
[25] F. Studer, A. Lebail, B. Raveau, J. Solid State Chem. 64 (1986) 414.
[26] V. Dimitrov, Y. Dimitriev, A. Montenero, J. Non-Cryst. Solids 180 (1994) 51.
[27] P. Pernice, A. Aronne, M. Catauro, A. Marotta, J. Non-Cryst Solids 210 (1997) 23.
[28] M.M. El-Desoky, S.M. Abo-Naf, J. Mater. Sci. Mater. Electron. 15 (2004) 425.
[29] C. Lin, J. Opt. Commun. 4 (1983) 2.
[30] M. Ferraris, D. Milanese, C. Contardi, Q. Chen, Y. Menke, J. Non-Cryst. Solids 347 (2004) 246.
[31] K. Nassau, D.L. Wood, D.K. Chadwick, Appl. Opt. 21 (1982) 4276.
[32] M.S. Metsik, T.I. Shishelova, G.F. Golovko, Z.N. Epifantseva, J. Appl. Spectrosc. 15 (2009) 1405.
[33] E. Culea, L. Pop, R. Muntean, M. Bosca, I. Bratu, M. Bogdan, Mod. Phys. Lett. B 21 (3) (2007) 1.
[34] S. Rada, E. Culea, J. Mol. Struct. 929 (2009) 141.
[35] K.N.R. Taylor, M.I. Darby, Physics of Rare Earth Solids, Chapman & Hall, London, 1972.
[36] O. Pinet, J. Phalippou, C. Di Nardo, J. Non-Cryst. Solids 352 (2006) 5382.
[37] B. Karthikeyan, S. Mohan, Physica B 334 (2003) 298.
[38] S. Simon, I. Ardelean, S. Filip, I. Bratu, I. Cosma, Solid State Commun. 116 (2000) 83.
[39] E. Culea, L. Pop, V. Simon, M. Neumann, I. Bratu, J. Non-Cryst. Solids 337 (2004) 62.
[40] E. Culea, L. Pop, S. Simon, Mat. Sci. Eng. B 112 (2004) 59.
[41] L.F. Bates, Modern Magnetism, Cambridge University Press, London, 1962, p. 133.
[42] E. Burzo, I. Ardelean, I. Ursu, Mater. Lett. 26 (1996) 103.
[43] C.M. Brodbeck, L.E. Iton, J. Chem. Phys. 83 (1985) 4285.
[44] J. Kliava, I.S. Edelman, A.M. Potseluyko, E.A. Petrakovskaja, R. Berger, I. Bruckental, Y. Yeshurun, A. Malakhovskii, T.V. Zarubina, J. Phys.: Condens. Matter 15 (2003) 6671.